Journal of the Serbian Society for Computational Mechanics / Vol. 15 / No. 2, 2021 / pp 93-100
(10.24874/jsscm.2021.15.02.09)

# FSI ANALYSIS WITH CONTINUOUS FLUID FLOW USING FEM AND SPH METHODS IN LS-DYNA

**Marko Topalović[1*], Aleksandar Nikolić[1], Snežana Vulović[1], Vladimir P. Milovanović[2]**

[1] Institute for Information Technologies, University of Kragujevac, Serbia
e-mail: topalovic@kg.ac.rs, dziga@kg.ac.rs, vsneza@kg.ac.rs
[2] Faculty of Engineering, University of Kragujevac, Serbia
e-mail: vladicka@kg.ac.rs
**corresponding author*

**Abstract**

The purpose of this research was to investigate the prospect of continuous flow modelling in LS-DYNA using SPH-FEM coupling. The both methods (SPH and FEM) are based on the continuum mechanics, however, SPH implementation uses Lagrangian material framework, while FEM uses an Eulerian formulation for the fluid analysis, and Lagrangian formulation for the solid analysis. The Lagrangian framework of the SPH means that we need to generate particles at one end, and to destroy them on the other, in order to generate a continuous fluid flow. The simplest way to do this is by using activation and deactivation planes, which is a solution implemented in the commercial LS- DYNA solver. Modelling of continuous fluid flow is practical in mechanical (naval) engineering for hydrofoil analysis and in bioengineering for blood vessel simulations. Results show that velocity fields obtained by SPH-FEM coupling are similar to velocity fields obtained by FEM. FEM only solution has a clear advantage in regards to execution time, however, SPH-FEM coupling offers greater insight into fluid structure interaction, that justifies the extra computational cost.

**Keywords:** SPH, FEM, Lagrangian formulation, Eulerian formulation, Fluid Structure Interaction, Hydrofoil, blood flow

## 1. Introduction

Smoothed Particle Hydrodynamics (SPH) is a mesh-free numerical method (Liu and Liu 2003), based on the continuum mechanics, which means that analyzed continuum is divided into sub-domains called pseudo-particles (Vignjević and Campbell 2011) that describe a certain section of material, fluid or solid, and not the individual real particles. It was originally designed for solving astrophysical problems (Gingold and Monaghan 1977), (Lucy 1977). Its purpose was later extended to Computational Fluid Dynamics (CFD) problems, governed by the Navier–Stokes equations (Monaghan and Pongracic 1985), and finally solid mechanics, by adding the strength of materials into SPH equilibrium equations (Libersky et al. 1993). SPH is also based on the Lagrangian material framework, meaning that the motion of the particular material section is observed (Liu and Liu 2003). On the other hand, when used for CFD analysis, FEM implements Eulerian spatial formulation which observes a fixed volume through which the fluid flows (Kojic

et al. 2009). Eulerian formulation can predict pressure and fluid velocity with great accuracy (Kojic et al. 2009), as well as forces exerted by the fluid on the surrounding vessel, but, if we want to observe the movements and interactions of particles within the fluid flow (Vignjević and Campbell 2011), we would still need a Lagrangian formulation.

Although fluid structure interaction is commonly studied using coupled SPH-FEM with fluid modelled with SPH particles and thin walled structure (aircraft fuselage or ship hull) modelled with FEM shell elements (Vignjević and Campbell 2011), these simulations are not done within the continuous fluid flow, the issue that we will address in this paper.

In the section 2 of this paper a brief retrospective of SPH kernel and particle approximation is given, along with the calculation of stress in viscous fluid. In the section 3 we will discuss flow generation in LS- DYNA (Hallquist 2006), and all of the problems we have encountered. Section 4 contains a practical implementation of the previously described methodology, demonstrated on hydrofoil analysis and hemodynamic analysis of blood vessels. Conclusion summarizes outcomes shown in this paper and points out ways to improve the continuous flow analysis using SPH which will be the focus of our further research.

## 2. SPH Fundamentals

SPH uses kernel approximation and particle approximation (Liu and Liu 2003) to model continuum matter for both solid and fluid, and these approximations will be briefly explained in this section, along with stress calculation in fluids.

### *2.1 Kernel approximation*

The conservation laws of continuum mechanics are expressed in the form of partial differential equations which are transformed into integral equations by interpolation function that gives "kernel estimate" of the field variables at point (Liu and Liu 2003). The exact value of the function $f(\mathbf{x})$ according to Liu and Liu (2003) in integral form is given with:

$$f(\mathbf{x}) = \int_{\Omega} f(\mathbf{x}')\delta(\mathbf{x}-\mathbf{x}')d\mathbf{x}', \tag{1}$$

where $f(\mathbf{x})$ is a function of position vector $\mathbf{x}$ defined in the domain $\Omega$ and $\delta(\mathbf{x}-\mathbf{x}') = \begin{cases} 1 & \mathbf{x} = \mathbf{x}' \\ 0 & \mathbf{x} \neq \mathbf{x}' \end{cases}$ is the Dirac delta measure (Liu and Liu 2003). Replacing $\delta(\mathbf{x}-\mathbf{x}')$ with bell-shaped kernel function $W(|\mathbf{x}-\mathbf{x}'|, h)$ where $h$ is the smoothing length (bell base radius), gives us a kernel approximation (Liu and Liu 2003) of function $f(\mathbf{x})$:

$$\langle f(\mathbf{x})\rangle = \int_{\Omega} f(\mathbf{x}')W(|\mathbf{x}-\mathbf{x}'|, h)d\mathbf{x}'. \tag{2}$$

### *2.2 Particle approximation*

The integral form given in Eq. (2) is not practical for numerical implementation because analysed continuum is divided into a finite number of particles which carry individual mass and occupy individual space, so Eq. (2) is converted to a discrete form of summation over all particles within

the support domain (Liu and Liu 2003). The infinitesimal volume $d\mathbf{x}'$ is replaced by finite volume of the particle $\Delta V_j = m_j / \rho_j$ where $m_j$ and $\rho_j$ are particle mass and particle density (Liu and Liu 2003). With the summation of all particles within support domain implemented in Eq. (2) we get particle approximation of a function $f(\mathbf{x})$ for particle *i*:

$$\langle f(\mathbf{x}_i)\rangle \cong \sum_{j=1}^{NNP} f(\mathbf{x}_j) W\left(\left|\mathbf{x}_i - \mathbf{x}_j\right|, h\right) dV_j = \sum_{j=1}^{NNP} \frac{m_j}{\rho_j} f(\mathbf{x}_j) W\left(\left|\mathbf{x}_i - \mathbf{x}_j\right|, h\right), \tag{3}$$

where NNP is the number of nearest neighbouring particles.

*2.3 SPH stress calculation in fluids*

Total stress tensor $\sigma_{\alpha\beta}$ in the viscous fluid (Vignjević and Campbell 2011) consists of the hydrostatic pressure $p$ and viscous stress ${}^{visc}\tau_{\alpha\beta}$:

$$\sigma_{\alpha\beta} = -p\delta_{\alpha\beta} + {}^{visc}\tau_{\alpha\beta}. \tag{4}$$

Viscous stress according to Liu and Liu (2003) can be calculated as:

$${}^{visc}\tau_{\alpha\beta} = \mu\left(\partial_a v_\beta + \partial_a v_\beta - \frac{2}{3}\partial_\gamma v_\gamma \delta_{\alpha\beta}\right) = \mu\varepsilon_{\alpha\beta}, \tag{5}$$

where $\mu$ is dynamic viscosity and $\varepsilon_{\alpha\beta}$ is the strain rate tensor (Liu and Liu 2003):

$$\varepsilon^i_{\alpha\beta} = \sum_{j=1}^{NNP} \frac{m_j}{\rho_j} v^{ji}_\beta \frac{\partial W^{ij}}{\partial x^i_\alpha} + \sum_{j=1}^{NNP} \frac{m_j}{\rho_j} v^{ji}_\alpha \frac{\partial W^{ij}}{\partial x^i_\beta} - \left(\frac{2}{3}\sum_{j=1}^{NNP} \frac{m_j}{\rho_j} \mathbf{v}^{ji} \cdot \nabla_i W^{ij}\right)\delta_{\alpha\beta}. \tag{6}$$

## 3. SPH fluid flow in LS-DYNA

Commercial LS- DYNA solver package (Hallquist 2006) is primarily used for crash simulations and dynamic analysis, while continuous fluid flow in SPH is not the main focus of research and development. For Incompressible Computational Fluid Dynamics (ICFD) LS- DYNA has a specific ICFD solver used for aerodynamics, hemodynamics, free-surface problems, ship hydrodynamics, etc. This solver uses an Eulerian formulation where incompressibility constraint may be applied. However, in this paper, we will focus on SPH solver of the LS- DYNA package and its potential for continuous fluid flow analysis. There are no examples, or published papers using this feature, however, in the manual (Hallquist 2006) there is a description of keywords BOUNDARY_SPH_FLOW and CONTROL_SPH (BOXID) that are used for activation and deactivation of SPH particles (Hallquist 2006), which can be used to create the continuous fluid flow. In this paper, we will test this feature on two sets of examples: one is hydrofoil, a structure similar to an airplane wing, which generates lift and raises the vessel hull over water, thus reducing the drag, and the other test case is simulation of blood flow in bioengineering. In all examples coupling between SPH and FEM methods is used, in the first case hydrofoil is modelled with shell FEM elements, and in the second case shell elements are used to model blood vessels. Schematics of these models are shown in Fig. 1.

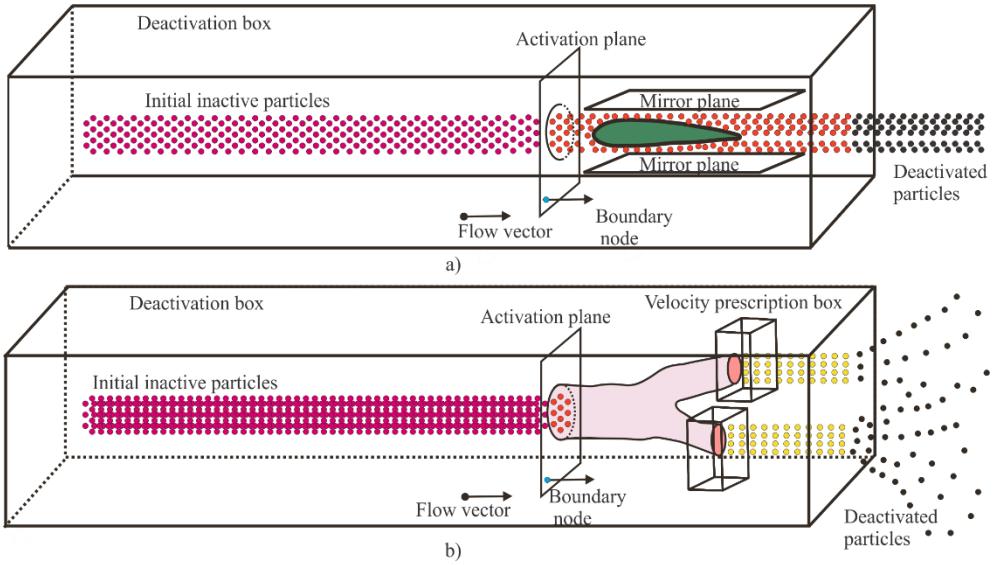


**Fig. 1.** SPH flow in LS-DYNA (a) Hydrofoil example, (b) Blood flow example.

This flow generation is similar to the activation and deactivation planes used by (Jonsson et al. 2011), and it also has some issues that we will now point out. First and foremost, the activation plane does not create new particles, it only activates them, so all of the particles that are going to flow through model, must be created before the analysis is started. Having most particles deactivated during the analysis saves computational time, but still deactivated particles make the model cumbersome. The same goes for the deactivation box, this boundary only flags SPH particles as inactive, they are no longer part of any calculation, but they are still there as a part of the model. BOUNDARY_SPH_FLOW keyword requires the prescription of node velocities for all of the particles centers i.e. inlet velocity. On the outlet side, we can define box which could prescribe node velocity of the exiting particles, but that velocity would need to be the same, i.e. we cannot define a parabolic velocity profile, unless we create a large number of boxes. Furthermore, if the model is too short, as we will see in the case of hydrofoil, the particles do not have enough space to even out their velocities. Without the velocity prescription box, the outlet is a free surface, which could make the model unrealistic. Another solution is to add new SPH part with sparse fixed particles to act like a sieve and to slow exiting particles down.

## 4. Analysis of results and discussion

### *4.1 SPH-FEM models of hydrofoils*

Hydrofoils are modelled as 2D problems, so we had to constrain translation of all particles in the direction normal to the observed plane. We used mirror SPH planes as boundary conditions (Hallquist 2006), but since these planes provide frictionless contact with ghost particles, we had to constrain two layers of particles on top and bottom in the flow direction to get more realistic behavior. We used two hydrofoil profiles to test the continuous fluid flow performance of SPH solver built in the commercial LS-DYNA program (Hallquist 2006). The first hydrofoil is a part of a high-speed passenger ship and its 1267 mm long with maximum thickness of 184 mm. Velocity of the ship i.e. inlet velocity of the model is 300 mm/s. SPH-FEM model has 8383 SPH particles, a number that includes 5280 initially deactivated particles, and 595 FEM elements.

FEM model used for comparison has 11974 elements and it is analyzed in PAKF solver (Kojic et al. 2009). The total analysis time is 2 s, with a time step of 0.01 s. Velocity field after 0.15 s shown in Fig. 2

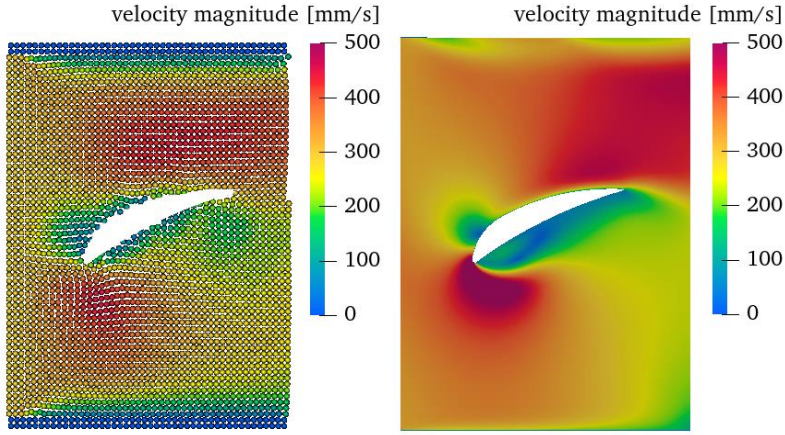


**Fig. 2.** Ship hydrofoil velocity field (a) SPH results, (b) FEM results.

The second hydrofoil is a part of a surfboard, and its 55.2 mm long with maximum thickness of 9.9 mm. SPH-FEM model has 11599 SPH particles, a number that includes 6000 initially deactivated particles, and 110 FEM elements. FEM model analyzed in PAKF (Kojic et al. 2009) used for comparison has 7070 elements. The total analysis time is 1 s, with a time step of 0.01 s, and inlet velocity of 300 mm/s. In the Fig. 3. we can see the velocity field for the surfboard hydrofoil at 0.2 s.

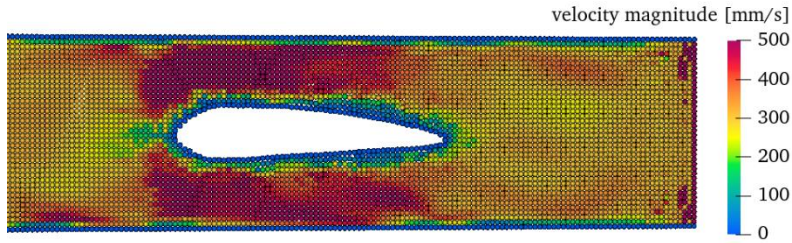


a)

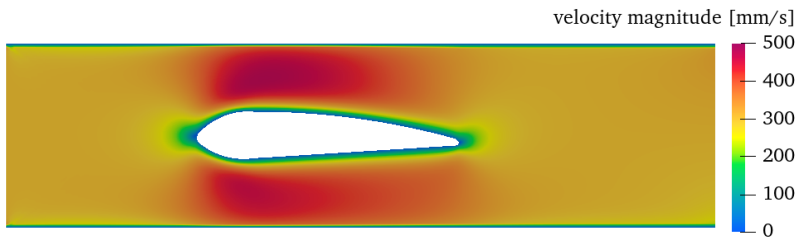


b)

**Fig. 3.** Surf board hydrofoil velocity field (a) SPH results, (b) FEM results.

As our analysis shows, slow moving hydrofoil with velocity of 300 mm/s cannot break the bonds between SPH particles in the boundary layer, so they slide over the contact surface. If the prescribed velocity is increased to 400 mm/s, the gap between SPH particles appear on top of the hydrofoil, which corresponds to the formation of the cavitation bubble nucleus (Roohi et al. 2013), Fig. 4.

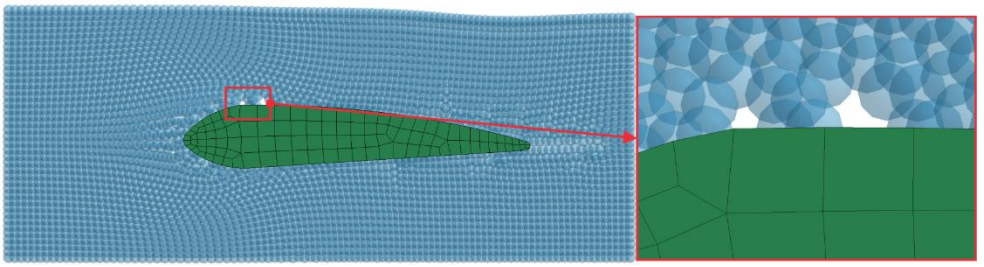

**Fig. 4.** Cavitation as gaps between SPH particles.

As it can be seen from Fig. 4. FEM-SPH coupling can be used to forecast location of formation of cavitation bubbles, but the full extent of the cavitation effect on the wetted surface cannot be predicted using these methods. In reality, decrease of velocity and increase of pressure of surrounding fluid causes the rapid collapse of cavitation bubbles which is followed by the great noise and occurrence of micro jets which can damage hydrofoil surface. In FEM-SPH coupled analysis, filling the gaps between SPH particles is not so sudden, and it does not create spikes in pressure on hydrofoil surface.

*4.2 SPH-FEM models of blood vessels*

The makeshift solution presented in this paper implies an initial set up of all of the particles which will be the part of the blood flow. To speed up the analysis, these particles move with the prescribed velocity and are excluded from the calculation until they pass through activation plane. On the other hand, when a particle passes through deactivation box, it's velocity and other state variables are no longer updated, and particle continue to fly away with a constant velocity, instead of getting completely deleted, which is a drawback of this solution. Inlet or outlet velocity for carotid bifurcation and artery with stenosis are prescribed according to the cardiac cycle value once particle coordinates are within the prescription box.

The actual carotid bifurcation model consists of 5180 SPH particles representing the blood, and 7692 shell FEM elements representing the blood vessel. In the Fig. 5 we can see particle velocities after 0.1 sec, and the paths that particles 34737 and 34810 had travelled in the first 0.1 sec.

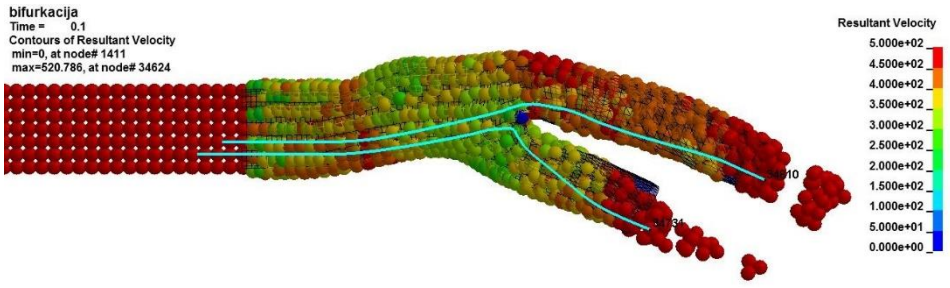


**Fig. 5.** Velocities in carotid bifurcation, LS-DYNA SPH results with particle path tracking.

Initially, these two particles were very close to each other at the inlet, but later, they got separated at bifurcation, and ended up flowing through different branches. Although in this case observed particles represent regular blood sections, SPH can easily handle a mixture of fluids or solid inclusions with different material properties. This path tracking can be used to study medicine distribution or cholesterol deposition in blood vessels.

Another test example is a blood vessel with stenosis, which consists of 2195 shell elements and 27417 SPH particles. In the Fig. 6 we can see particle velocities after 0.452 sec, and the path that particle 10166 had travelled inside observed section of the vessel. After entering the vortex, the observed particle has partially circular, partially chaotic movement, until it eventually frees itself from the vortex and continue to flow out of the observed blood vessel.

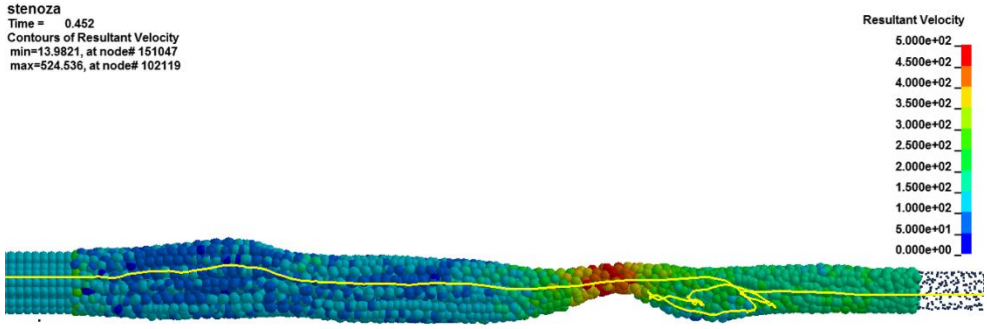


**Fig. 6.** Velocity magnitude inside of blood vessel with stenosis, LS-DYNA path tracking shows particle movement within the vortex.

Demonstrated methodology is applicable in both mechanical and bioengineering, however, we must point out that this solution is not the state of the art, for example, open source SPH solver DualSphysics (Domínguez et al. 2021) has an inlet/outlet prescription, and although that procedure represents the next level in comparison to LS-DYNA, it still has many challenges that are the study focus of several research groups. To name a few, pressure prescription developed by Holmes and Pivonka (2021), permeable and non-reflective boundaries which are works of (Lastiwka et al. 2009) and open boundaries implemented by Vacondio et al. (2012).

## 5. Conclusions

SPH method coupled with FEM is often used in maritime engineering to predict fluid-structure interaction between vessels and surrounding water. However, these calculations are usually done with static water, and vessels that impact water at high speeds. In this paper, we analyzed SPH-FEM coupling for FSI analysis of a continuous fluid flow. The obtained results are similar to those obtained by Eulerian FEM analysis, but the prescription of boundaries is much more difficult in LS-DYNA with coupled SPH-FEM solvers. Execution time is also significantly longer for SPH-FEM analysis. On the other hand, SPH coupled with FEM can be used as a prediction tool for the location where the cavitation will occur, but not to model the damage it causes. SPH has a great potential to be used in the maritime industry for analysis of impact of floating bodies on vessels, but to realize its full potential, boundary conditions for generation and destruction of SPH particles need to be implemented, in order to simulate continuous fluid flow. Elaborate prescription of boundary conditions in LS-DYNA is used in Bioinformatics to mimic such behaviour for hemodynamic analysis, however, this requires initial modelling of all SPH

particles which will flow through blood vessel, and on the outlet of the vessel, deactivated particles continue to fly away with constant velocity, ever increasing simulation space.

**Acknowledgement:** This research is supported by the Ministry of Education, Science and Technological Development, Republic of Serbia, Grant TR32036 and 451-03-9/2021-14/200378.

## References

Domínguez M, Fourtakas G, Altomare C, Canelas R, Tafuni A, García-Feal O, Martínez-Estévez O, Mokos A, Vacondio R, Crespo A, Rogers B, Stansby P, Gómez-Gesteira M. (2021). DualSPHysics: from fluid dynamics to multiphysics problems, *Comp. Part. Mech.*

Gingold A, Monaghan J (1977). Smoothed particle hydrodynamics: theory and application to non-spherical stars, *Mon. Notices Royal Astron. Soc.*, 181, 375-389.

Jonsson P, Jonsén P, Andreasson P, Hellström I, Lundström S (2011). Smoothed Particle Hydrodynamics Modeling of Hydraulic Jumps, Proc. Particle-Based Methods II—Fundamentals and Applications, Barcelona, Spain.

Hallquist O (2006). *LS-DYNA Theory Manual*. Livermore Software Technology Corporation.

Holmes D, Pivonka P (2021). Novel pressure inlet and outlet boundary conditions for Smoothed Particle Hydrodynamics, applied to real problems in porous media flow *J. Comput. Phys.*, 429, 110029

Kojic M, Filipovic N, Stojanovic B, Kojic N (2009). *Computer Modeling in Bioengineering: Theoretical Background, Examples and Software*, John Wiley & Sons.

Lastiwka M, Basa M, Quinlan N (2009) Permeable and non-reflecting boundary conditions in SPH, Int. J. Numer. Methods Fluids. 61.709–724.

Libersky D, Petschek G, Carney C, Hipp R, Allahdadi A (1993) High Strain Lagrangian Hydrodynamics: A Three-Dimensional SPH Code for Dynamic Material Response, J. Comput. Phys., 109. 67-75.

Liu G, Liu M (2003). *Smoothed Particle Hydrodynamics*, World Scientific Publishing.

Lucy B (1977). A numerical approach to the testing of fusion process, *Astron. J.*, 88, 1013-1024.

Monaghan J, Pongracic H (1985). Artificial viscosity for particle methods, *Appl. Numer. Math.*, 1, 187-194.

Roohi E, Zahiri P, Passandideh-Fard M (2013). Numerical simulation of cavitation around a two-dimensional hydrofoil using VOF method and LES turbulence model, *Appl. Math. Model.*, 37, 6469–6488.

Vacondio R, Rogers B, Stansby P, Mignosa P (2012). SPH Modeling of Shallow Flow with Open Boundaries for Practical Flood Simulation, *J. Hydraul. Eng.*, 138. 530–541.

Vignjević R, Campbell J (2011). Brief review of development of the smooth particle hydrodynamics (SPH) method. Proc. IConSSM 2011 - The 3rd International Congress of Serbian Society of Mechanics, Vlasina lake, Serbia.